# Additive Manufactured Matching Medium Design for Implant Communications

Ozum Habiboglu*, Sila Akgun †, Erdem Cil *, Ozlem Aydin Civi †, Sema Dumanli *
*Electrical and Electronics Engineering Dept., Bogazici University, Istanbul, Turkey, sema.dumanli@boun.edu.tr
†Electrical-Electronics Engineering Dept., Middle East Technical University, Ankara, Turkey, ozlem@metu.edu.tr

***Abstract*—The design of matching media with different dielectric constants for the use in implant communications is presented in this paper. Each medium consists of a three-dimensional printed honeycomb structure filled with a high dielectric lossless semi-liquid. The dielectric constant of the media is determined by the infill percentage of the honeycomb structure as well as the dielectric constant of both the semi-liquid and the material of the structure. An algorithm is developed that can specify values for the infill percentage to reach a target dielectric constant value from a given material and semi-liquid. For the measurements, several honeycomb structures with different infill percentages are fabricated with polylactic acid using additive manufacturing. Water-based semi-liquids are developed to fill the structures. The dielectric constants of the fabricated media are measured with a half-filled rectangular resonant cavity. The practical results indicate that target dielectric constants ranging from 8 to 34 are reached by using semi-liquids with dielectric constants ranging from 20 to 65. The practical results are also shown to be in good agreement with the numerical ones with an error of less than 9% for all different cases.**

***Index Terms*—cavity resonators, dielectric constant, implants, three-dimensional printing.**

## I. Introduction

Implant devices are frequently used in medical applications, particularly for the purpose of diagnosis and treatment of a disease [1]. Besides the fact that millions of people around the world rely already on the current implantable medical devices to maintain the quality of their daily life, new implantable devices are also being developed for medical applications. Therefore, as technological advancement continues, the use of implantable devices in the field of medicine is predicted to increase rapidly in the near future [2].

An antenna implanted inside the human body is surrounded by lossy human tissues most of which have high dielectric constant and high conductivity [3]. The difference between the dielectric constants of air and the human tissues gives rise to the reflection of electromagnetic (EM) waves from the air-tissue boundary [4]. This phenomenon introduces a challenge for implant communications, as it may lead to a significant reduction in the overall efficiency of the wireless link. To overcome this challenge, a medium of which the dielectric constant can be adjusted to a value greater than that of air and lower than that of the tissue can be placed between the antenna and the tissue. Such a medium is referred to as a matching medium and can be considered as a middle medium for the propagation of EM waves. Moreover, the reflections from the air-tissue boundary can further be reduced with the use of a matching medium of which the dielectric constant gradually changes. A matching medium with gradually changing dielectric constant can easily be realized with additive manufacturing (AM).

As it provides the designers with a great deal of flexibility in the manufacture of three-dimensional (3D) structures [5], AM, a technique consisting of numerous processes that make use of materials added together to manufacture 3D structures [6], is one of the techniques commonly preferred in the literature to adjust the dielectric constants of structures fabricated from a bulk material. In [7], several 3D printed samples with different infill percentages, where the voids are filled with air, are fabricated from an Acrylonitrile-Butadiene-Styrene (ABS) filament and the effect of the infill percentages on the dielectric constant is examined. Similarly in [8] and [9], 3D printed samples with different infill percentages are fabricated from a Ninjaflex filament and the dielectric constants of the different samples are measured using a waveguide and a ring-resonator, respectively. In [10], various 3D printed composites that consist of an ABS filament loaded with different fractions of barium titanate (BaTiO3) are presented and the dielectric constants of these composites are given. Finally in [11], the authors propose a multi-zone lens antenna that is optimized by controlling the dielectric constant using additive manufacturing. Here, to the best of authors' knowledge, additive manufacturing has been utilized to realize a matching medium for the first time in the literature.

In this work, the design of matching media that include a 3D printed honeycomb structure filled with high dielectric lossless semi-liquids (HDLSL) is presented. The numerical analysis of the media is performed and a set-up is prepared to measure the dielectric constants of the manufactured media. In Section II, the honeycomb structure and the algorithm used for the calculation of the target dielectric constants are described. The measurement set-up used to determine the dielectric constants of the fabricated media is explained in Section III. The numerical and practical results for the target dielectric constants are compared and interpreted in Section IV. Finally, Section V concludes the work.

## II. Design of the Matching Medium

In this paper, an easily printable, uniform pattern with a simple geometry is selected as the matching medium. The 3D printed structure is chosen to be a honeycomb structure consisting of repeating hexagon patterns as visualized in Fig. 1, as

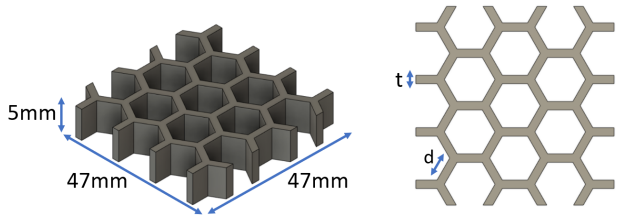


Fig. 1. Isometric view (left) and top view (right) of an example honeycomb structure. t: wall thickness, d: hexagon side length of the honeycomb structure.

it enables the infill percentage to be tuned easily by changing the wall thickness and the side length of the structure. In addition, with a fixed honeycomb wall thickness, the structure infill percentage can be altered when the side length is changed unlike a repeating square pattern. The calculation of target dielectric constants of the media are carried out step by step. In the first step, to perform numerical analyses, the honeycomb structures are imported to ANSYS High Frequency Structure Simulator (HFSS) [12]. The numerical matching media are completed in HFSS by filling the hexagonal voids in each structure with solid structures (HDLSLs) as visualized in Fig. 2. During the numerical analyses, the dielectric constant of each honeycomb structure is changed from 1 to 9 in increments of 1, while that of the HDLSLs ranges from 10 to 80 in increments of 5. Next, the media are enclosed by perfect electric conductor planes forming a rectangular resonant cavity totally filled with the matching medium. The lowest resonant frequency in each case is determined by using the Eigenmode as the solution type in HFSS and tabulated separately. As there are 4 different wall thicknesses and 9 different dielectric constants for the honeycomb structures, 36 tables of the resonant frequency are prepared in total. Finally, as the resonant frequencies of a rectangular cavity is given as in (1) [13], the dielectric constants of the media can be calculated using (2). The calculated dielectric constants are tabulated (36 separate tables) as illustrated in Table I.

$$f_{mnp} = \frac{c}{2\sqrt{\epsilon_r \mu_r}} \sqrt{\left(\frac{m}{a}\right)^2 + \left(\frac{n}{b}\right)^2 + \left(\frac{p}{h}\right)^2} \quad (1)$$

$$\epsilon_r = \left[\frac{c}{2 f_{mnp}\sqrt{\mu_r}} \sqrt{\left(\frac{m}{a}\right)^2 + \left(\frac{n}{b}\right)^2 + \left(\frac{p}{h}\right)^2}\right]^2 \quad (2)$$

In the second step, an algorithm is developed that makes use of prepared dielectric constant tables to calculate the required infill percentage of a structure to reach a target dielectric constant from a given material and HDLSL. The infill percentage indicates the ratio of the top-view area of the honeycomb structure to its total top-view area and is determined by the wall thickness and side length values. The inputs of the developed algorithm are the target dielectric constant and the dielectric constant of the material and the HDLSL. Note that numerically determined dielectric constants of the media (Table I) are calculated only for integer values

TABLE I

THE DIELECTRIC CONSTANTS OF THE MEDIA FOR A WALL THICKNESS OF 1 MM AND MATERIAL $\epsilon_r$ = 2 THAT ARE CALCULATED BY SUBSTITUTING THE LOWEST RESONANT FREQUENCY OF A RECTANGULAR CAVITY TOTALLY FILLED WITH THE MEDIA INTO EQUATION 2

| HDLSL | Hexagon Side Length (mm) | | | | | | | | | |
|---|---|---|---|---|---|---|---|---|---|---|
| $\epsilon_r$ | 2 | 2.5 | 3 | 3.5 | 4 | 4.5 | 5 | 6 | 7 | 8 |
| 10 | 6.8 | 7.3 | 7.6 | 7.9 | 8.1 | 8.3 | 8.4 | 8.7 | 8.8 | 9.0 |
| 15 | 9.8 | 10.6 | 11.2 | 11.6 | 11.9 | 12.2 | 12.5 | 12.8 | 13.1 | 13.3 |
| 20 | 12.9 | 13.9 | 14.7 | 15.3 | 15.8 | 16.2 | 16.5 | 17.0 | 17.4 | 17.7 |
| 25 | 15.9 | 17.2 | 18.2 | 19.0 | 19.6 | 20.1 | 20.5 | 21.2 | 21.6 | 22.0 |
| 30 | 18.9 | 20.5 | 21.7 | 22.7 | 23.4 | 24.0 | 24.5 | 25.3 | 25.9 | 26.4 |
| 35 | 21.9 | 23.8 | 25.2 | 26.3 | 27.2 | 28.0 | 28.6 | 29.5 | 30.2 | 30.8 |
| 40 | 24.9 | 27.1 | 28.8 | 30.0 | 31.0 | 31.9 | 32.6 | 33.6 | 34.5 | 35.1 |
| 45 | 27.9 | 30.4 | 32.3 | 33.7 | 34.9 | 35.8 | 36.6 | 37.8 | 38.7 | 39.5 |
| 50 | 30.9 | 33.7 | 35.8 | 37.4 | 38.7 | 39.7 | 40.6 | 42.0 | 43.0 | 43.8 |
| 55 | 34.0 | 37.0 | 39.3 | 41.1 | 42.5 | 43.7 | 44.7 | 46.1 | 47.3 | 48.2 |
| 60 | 37.0 | 40.3 | 42.8 | 44.8 | 46.3 | 47.6 | 48.7 | 50.3 | 51.5 | 52.6 |
| 65 | 40.0 | 43.6 | 46.4 | 48.5 | 50.2 | 51.5 | 52.7 | 54.5 | 55.8 | 56.9 |
| 70 | 43.0 | 46.9 | 49.9 | 52.2 | 54.0 | 55.5 | 56.7 | 58.6 | 60.1 | 61.3 |
| 75 | 46.0 | 50.2 | 53.4 | 55.9 | 57.8 | 59.4 | 60.8 | 62.8 | 64.4 | 65.6 |
| 80 | 49.0 | 53.5 | 56.9 | 59.6 | 61.6 | 63.3 | 64.8 | 67.0 | 68.6 | 70.0 |

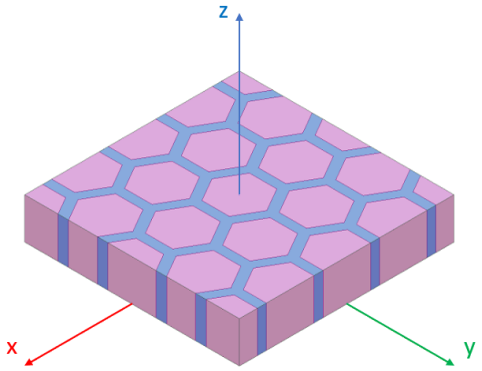


Fig. 2. An example of a completed numerical matching medium (Blue: honeycomb structure with t = 2 mm, d = 6 mm, Pink: HDLSL filling the voids).

of material $\epsilon_r$ from 1 to 9. Firstly, the algorithm uses these tables to generate a new table similar to Table I for a given non-integer material $\epsilon_r$. For this generation, the corresponding data in the tables belonging to the nearest integers that are greater and smaller than given $\epsilon_r$ are used as upper and lower boundaries, respectively. Next, the new data are generated such that the difference between the generated data and the upper and lower boundaries is directly proportional to the difference between the given $\epsilon_r$ and the greater and smaller integer $\epsilon_r$, respectively. To illustrate, the new values generated by the algorithm for polylactic acid (PLA) with $\epsilon_r$ = 2.7 and a HDLSL with $\epsilon_r$ = 50 are marked with crosses $(\times)$ in the

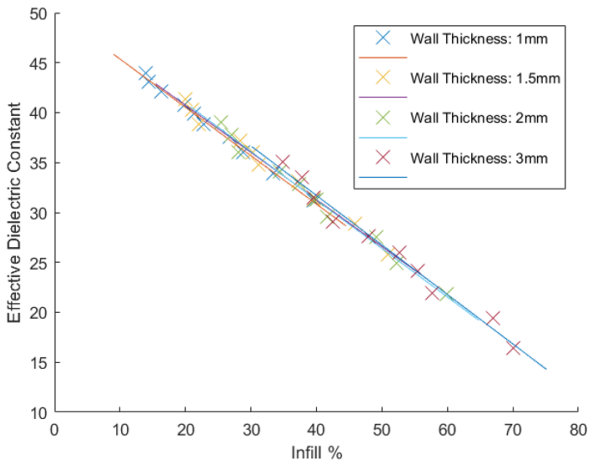


Fig. 3. Target dielectric constant vs.infill % graph for PLA ($\epsilon_r$ = 2.7) filled with a HDLSL with $\epsilon_r$ = 50. The crosses show the new values generated by the developed algorithm and the straight lines are the lines fitted with the new values.

graph given in Fig. 3. As the dielectric constant of the HDLSLs is greater than that of the materials, the dielectric constant of the medium decreases as the infill percentage increases. Later, the algorithm fits a curve to the generated data. As can be seen from Fig. 3, the generated data are almost linearly distributed. Hence, linear regression, which is commonly used to fit the data to a model in the context of machine learning, is used to create a continuous graph of infill percentage vs. dielectric constant. The equations used by linear regression can be summarized as

$$n = length(x) = length(y) \tag{3}$$

$$a_1 = \frac{n\sum(xy^T) - \sum x \sum y}{n\sum(xx^T) - (\sum x)^2} \tag{4}$$

$$a_0 = mean(y) - a_1 mean(x) \tag{5}$$

$$y = a_1 x + a_0. \tag{6}$$

Finally, using the fitted line, the algorithm determines the infill percentage required for a target dielectric constant and gives it as an output along with the corresponding side lengths for distinct wall thicknesses as shown in Fig. 4. Note that, although the infill percentages can be mapped to precise t and d values of a honeycomb structure, precision of 3D printers must also be considered. For that reason, the required infill percentage is rounded to the infill percentage of the nearest previously prepared model, then its t and d values are given as outputs. In some cases, infill percentage of a model with certain t may be much smaller than the desired infill percentage (or the opposite). In those cases, "Nan" is given as the output. Lastly, even though no numerical analysis is performed for t = 4 mm and t = 5 mm, their dielectric constant can be estimated based on their infill percentages, as the infill percentage determines the dielectric constant. The final results for PLA with t = 2 mm and t = 3 mm are tabulated in Table II.

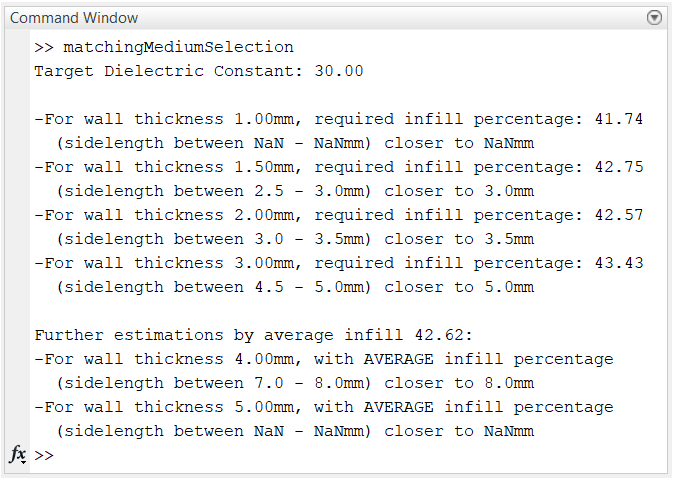


Fig. 4. The output of the algorithm showing the required infill percentages to reach the target dielectric constant from an HDLSL with $\epsilon_r$ = 50 for PLA.

TABLE II
REQUIRED WALL THICKNESSES AND SIDE LENGTHS FOR PLA TO REACH DIFFERENT TARGET DIELECTRIC CONSTANTS FROM A GIVEN HDLSL

| HDLSL $\epsilon_r$ | Target $\epsilon_r$ | Wall thickness (mm) | Side Length (mm) | Sample Number |
|---|---|---|---|---|
| 65 | 46.7 | 2 | 6 | #19 |
| | 38.1 | 2 | 3.5 | #18 |
| | 28.0 | 3 | 3 | #17 |
| | 27.9 | 2 | 2 | #16 |
| 62 | 41.4 | 3 | 7 | #15 |
| | 36.4 | 2 | 5 | #14 |
| | 32.0 | 3 | 4 | #13 |
| | 30.6 | 2 | 2.5 | #12 |
| | 20.0 | 3 | 2 | #11 |
| 48 | 27.9 | 3 | 5 | #10 |
| | 28.4 | 2 | 3.5 | #9 |
| | 18.7 | 3 | 2.5 | #8 |
| 42 | 30.4 | 2 | 6 | #7 |
| | 25.0 | 2 | 3.5 | #6 |
| | 21.2 | 2 | 2.5 | #5 |
| 34 | 23.1 | 3 | 7 | #4 |
| | 22.6 | 2 | 4.5 | #3 |
| 20 | 8.8 | 3 | 3 | #2 |
| | 9.6 | 2 | 2 | #1 |

## III. HDLSL DEVELOPMENT AND MEASUREMENT SET-UP

In order to measure the dielectric constants of different matching media, HDLSLs are developed. The developed HDLSLs are water-based HDLSLs that are prepared using deionized water, canola oil, Cetrimonium bromide (CTAB), cornstarch and propylene glycol. The amount of each ingredient required to reach specified dielectric constant values are tabulated in Table III. The dielectric constants of the HDLSLs are determined by the ratio of the deionized water ($\epsilon_r$ = 80) to the canola oil ($\epsilon_r$ = 3). CTAB is the emulsifier, corn starch is the solidifier and propylene glycol is the stabilizer. The

TABLE III
THE AMOUNT OF EACH INGREDIENT USED FOR SPECIFIED DIELECTRIC CONSTANTS

| | Dielectric Constant | | | | | |
|---|---|---|---|---|---|---|
| | 20 | 34 | 42 | 48 | 62 | 65 |
| Deionized Water (g) | 110 | 110 | 100 | 100 | 125 | 165 |
| Canola Oil (g) | 30 | 30 | 20 | 15 | 10 | 10 |
| Cornstarch (g) | 45 | 34 | 20 | 15 | 20 | 20 |
| CTAB (ml) | 3 | | | | | |
| Propylene Glycol (g) | 1 | | | | | |

dielectric constants of the developed HDLSLs are measured using an in-house open-ended coaxial cable model with an accuracy of 95% [14].

The honeycomb structures given in Table II are fabricated with PLA using additive manufacturing. Several of the fabricated structures are shown in Fig. 5a. Each structure is filled with the prepared HDLSLs as seen in Fig. 5b. The measurements are taken with a 5 cm $\times$ 5 cm $\times$ 1 cm rectangular cavity resonator as visualized in Fig. 5c. Each medium is placed into the cavity separately, resulting in a half-filled cavity as shown in Fig. 5d, and the lowest resonant frequency of the cavity is measured in each case. The half-filled cavity is preferred to ease the excitation. The dielectric constant of the media is determined according to the lowest resonant frequency of the cavity.

## IV. Results and Discussion

Fig. 6 shows the simulation results obtained from HFSS and the measurement results for different matching media tabulated in Table II along with the percentage error between them. Blue columns indicate the simulation results, whereas orange columns indicate the measurement results. As can be seen, the measurement results are in good agreement with the simulated ones. The calculated percentage error between the simulation and measurement results are less than 9% in each case. This disagreement is estimated to result from the inaccuracies during the manufacturing process such as the unintended voids left inside the manufactured structure or the precision of the 3D printer. Nevertheless, the disagreement between the simulation and measurement results is found to be acceptable.

As can be seen from Fig. 6, a target dielectric constant interval from 8 to 34 is reached with high accuracy by using HDLSLs with dielectric constants ranging from 20 to 65. This result indicates that any target dielectric constant required for a matching medium used for in-body communications can be reached using this technique. It also provides a guide to create a matching medium that has gradually increasing dielectric constant towards the human body.

## V. Conclusion

Matching media with different dielectric constants are designed with 3D printed honeycomb structures and HDLSLs.

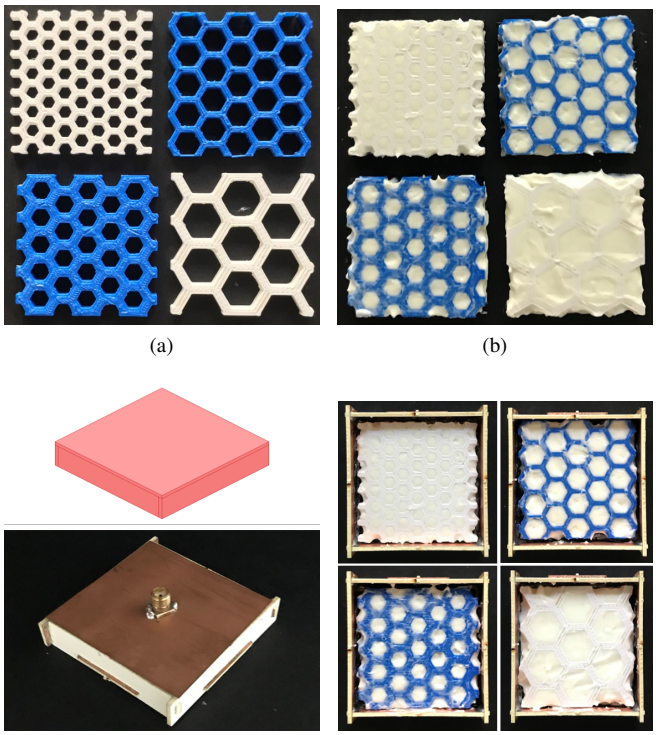

Fig. 5. Manufactured honeycomb structures and the cavity used in the measurements (a) structures with empty voids (b) structures filled with HDLSL (c) numerical (up) and physical (down) rectangular cavity (d) structures placed into the cavity.

The physical parameters of the honeycomb structures are calculated for different target permittivity values with a developed algorithm. The honeycomb structures are fabricated using additive manufacturing and water-based HDLSLs are developed for the measurements. The numerical results are validated with the measurements taken in a rectangular resonant cavity. In the light of the measurement results, the proposed matching medium design is shown to cover a dielectric constant interval from 8 to 34 with an error of less than 9%. In the future, the authors aim to create matching media with gradually changing dielectric constants in order to increase the transmitted power into the human body.

## Acknowledgment

This study is financially supported by Bogazici University Research Fund under project number 14543.

## References

[1] A. K. Skrivervik and F. Merli, "Design strategies for implantable antennas," in *2011 Loughborough Antennas Propagation Conference*, pp. 1–5, Nov 2011.

[2] A. Kiourti and K. S. Nikita, "A review of implantable patch antennas for biomedical telemetry: Challenges and solutions [wireless corner]," *IEEE Antennas and Propagation Magazine*, vol. 54, no. 3, pp. 210–228, 2012.

[3] T. Dissanayake, K. P. Esselle, and M. R. Yuce, "Dielectric loaded impedance matching for wideband implanted antennas," *IEEE Transactions on Microwave Theory and Techniques*, vol. 57, no. 10, pp. 2480–2487, 2009.

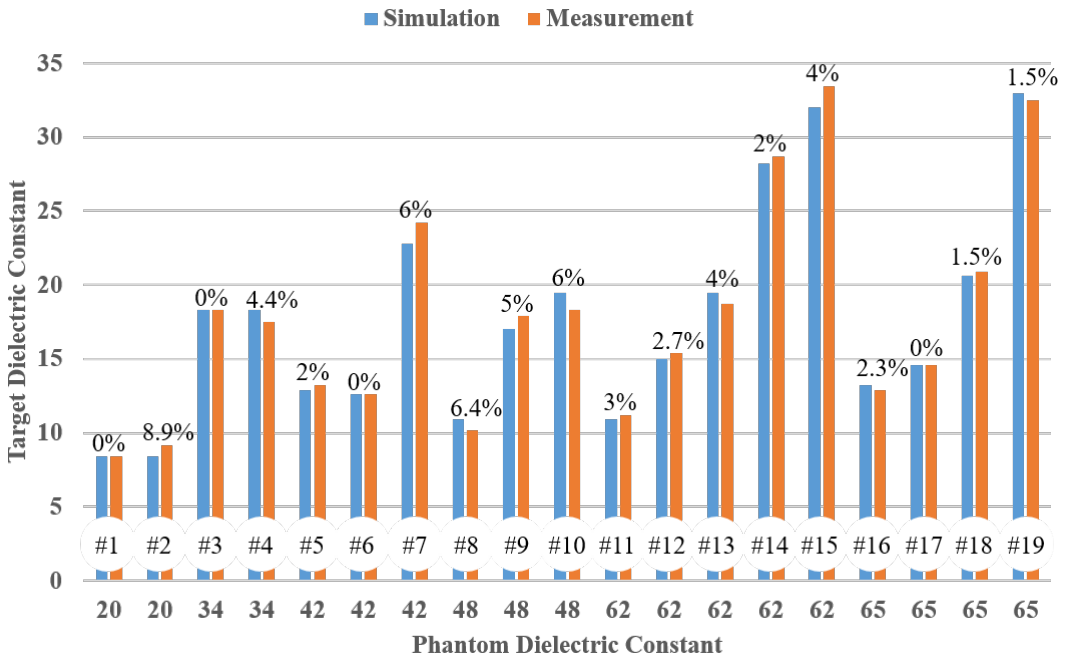


Fig. 6. Simulation and measurement results for different matching media given in Table II. The percentages given above the columns indicate the corresponding percentage errors between the simulation and measurement results.


[4] H. Lui, A. Fhager, and M. Persson, "Matching medium for biomedical microwave imaging," in *2015 International Symposium on Antennas and Propagation (ISAP)*, pp. 1–3, 2015.

[5] A. Goulas, S. Zhang, D. Cadman, J. Järveläinen, V. Mylläri, J. Y. Vardaxoglou, and D. Engstrom, "The impact of 3d printing process parameters on the dielectric properties of high permittivity composites," *Designs*, vol. 4, 11 2019.

[6] H. Lhachemi, A. Malik, and R. Shorten, "Augmented reality, cyber-physical systems, and feedback control for additive manufacturing: A review," *IEEE Access*, vol. 7, pp. 50119–50135, 2019.

[7] B. Biernacki, S. Zhang, and W. Whittow, "3d printed substrates with graded dielectric properties and their application to patch antennas," in *2016 Loughborough Antennas Propagation Conference (LAPC)*, pp. 1–5, 2016.

[8] E. Massoni, L. Silvestri, M. Bozzi, L. Perregrini, G. Alaimo, S. Marconi, and F. Auricchio, "Characterization of 3d-printed dielectric substrates with different infill for microwave applications," in *2016 IEEE MTT-S International Microwave Workshop Series on Advanced Materials and Processes for RF and THz Applications (IMWS-AMP)*, pp. 1–4, 2016.

[9] R. Bahr, T. Le, M. M. Tentzeris, S. Moscato, M. Pasian, M. Bozzi, and L. Perregrini, "Rf characterization of 3d printed flexible materials - ninjaflex filaments," in *2015 European Microwave Conference (EuMC)*, pp. 742–745, 2015.

[10] F. Castles, D. Isakov, A. Lui, Q. Lei, C. Dancer, Y. Wang, J. Janurudin, S. Speller, C. Grovenor, and P. Grant, "Microwave dielectric characterisation of 3d-printed batio3/abs polymer composites," *Scientific Reports*, vol. 6, p. 22714, 03 2016.

[11] J. M. Monkevich and G. P. Le Sage, "Design and fabrication of a custom-dielectric fresnel multi-zone plate lens antenna using additive manufacturing techniques," *IEEE Access*, vol. 7, pp. 61452–61460, 2019.

[12] *ANSYS High Frequency Structure Simulator (HFSS)*. Oct. 2020. [Online]. Available: https://www.ansys.com/products/electronics/ansys-hfss.

[13] D. M. Pozar, *Microwave engineering*. John wiley & sons, 2009.

[14] F. M. Ghannouchi and R. G. Bosisio, "Measurement of microwave permittivity using a six-port reflectometer with an open-ended coaxial line," *IEEE Transactions on Instrumentation and Measurement*, vol. 38, no. 2, pp. 505–508, 1989.